Flow Visualization of Oscillation Characteristics of Liquid and Vapor Flow in the Oscillating Capillary Tube Heat Pipe

Jong–Soo Kim*

School of Mechanical Engineering, Pukyong National University,
San 100, Yongdang dong, Nam–gu, Pusan 608–737, Korea

Ngoc Hung Bui

Graduate student, School of Mechanical Engineering, Pukyong National University,
San 100, Yongdang dong, Nam–gu, Pusan 608–737, Korea

Ju–Won Kim

LG Electronics Co. Ltd, 76, Seongsan–Dong, Changwon City, Gyeongnam, 641–713, Korea

Jeong–Hoon Kim, Hyun–Seok Jung

Samsung Electronics Co. Ltd, 416,
Maetan–3Dong, Paldal–Gu, Suwon City, Kyungki–Do, 442–742, Korea

The two–phase flow patterns for both non–loop and loop type oscillating capillary tube heat pipes (OCHPs) were presented in this study. The detailed flow patterns were recorded by a high–speed digital camera for each experimental condition to understand exactly the operation mechanism of the OCHP. The design and operation conditions of the OCHP such as turn number, working fluid, and heat flux were varied. The experimental results showed that the representative flow pattern in the evaporating section of the OCHP was the oscillation of liquid slugs and vapor plugs based on the generation and growth of bubbles by nucleate boiling. As the oscillation of liquid slugs and vapor plugs was very speedy, the flow pattern changed from the capillary slug flow to a pseudo slug flow near the annular flow. The flow of short vapor–liquid slug–train units was the flow pattern in the adiabatic section. In the condensing section, it was the oscillation of liquid slugs and vapor plugs and the circulation of working fluid. The oscillation flow in the loop type OCHP was more active than that in the non–loop type OCHP due to the circulation of working fluid in the OCHP. When the turn number of the OCHP was increased, the oscillation and circulation of working fluid was more active as well as forming the oscillation wave of long liquid slugs and vapor plugs in the OCHP. The oscillation flow of R–142b as the working fluid was more active than that of ethanol and the high efficiency of the heat transfer performance of R–142b was achieved.

Key Words : Oscillating Capillary Tube Heat Pipe (OCHP), Two–Phase Flow Patterns, Flow Oscillation

1. Introduction

* Corresponding Author,
  E-mail : jskim@pknu.ac.kr
  TEL : +82-51-620-1502; **FAX** : +82-51-611-6368
  School of Mechanical Engineering, Pukyong National
  University, San 100, Yongdang dong, Nam-gu, Pusan
  608-737, Korea. (Manuscript **Received** October 10,
  2002; **Revised** March 11, 2003)

The oscillating capillary tube heat pipe (OCHP) is a very promising heat transfer device (Akachi, 1994). In addition to its excellent heat transfer performance, it has a simple structure: in contrast with conventional heat pipes, there is no wick structure to return the condensed working fluid

back to the evaporating section. The OCHP is made from a long continuous capillary tube bent into many turns of a serpentine structure. The working fluid is charged into the OCHP. The diameter of the OCHP must be sufficiently small so that vapor plugs can be formed by capillary action. The OCHP is operated within a 0.1~5 mm inner diameter range. The OCHP can operate successfully for all heating modes. The heat input, which is the driving force, increases the pressure of the vapor plugs in the evaporating section. In turn, this pressure increase will push neighboring vapor plugs and liquid slugs toward the condensing section, which is at a lower pressure. However, due to the continuous heating, small bubbles formed by nucleate boiling grow and coalescence to become vapor plugs. The flow of vapor plugs and liquid slugs moves to the condensing section by pressure difference. The heat transfer continuously occurs. As a result, thermal energy is rapidly transferred from the evaporating section to the condensing section as well as the oscillation and circulation of liquid slugs and vapor plugs occurring in the OCHP (Akachi et al., 1994, 1996).

Both experimental and numerical investigations on OCHPs have been carried out by some researchers. The experiments mainly focus on the visualization of flow pattern and the measurement of temperature and effective thermal conductivity. Takahashi et al.(1998) conducted flow visualization experiments using the proton radiography method on the aluminum-extruded type OCHP. The cross section of flow channels was rectangular of 0.6 mm×0.7 mm. The working fluid used was R-134a at the charging ratio of 30 vol.%. They concluded that the flow pattern depends on the inlet heat flux and inclination angle of the test section. However, in their study, the detailed flow pattern could not be understood due to the indirectly projected flow pattern. Nishio and Hosoda et al.(1997) considered the regularity of flow pattern according to the charging ratio of working fluid. The OCHP of 10 turns was made of glass tubes (inner diameter of 2.4 mm) and the used working fluid was distilled water. They reported that as the charging ratio was decreased,

the movement of liquid columns was irregular and their experimental results agreed well with the numerically simulated flow pattern. Numata et al.(1999) investigated flow visualization experiments according to the variation of tube diameter. The glass tube type OCHPs (of 2.4 mm and 5 mm inner diameters) were used and the working fluids were water and R-141b. They concluded that as the tube diameter was increased, the flow pattern changed from slug flow to churn flow and annular flow. However, the experimental results obtained in their study were somewhat different from the flow pattern in the metal tube because the glass tubes of low thermal conductivity were used. Gi et al.(1999) observed flow pattern according to the charging ratio of working fluid, the operation temperature and inclination angle of the OCHP of 10 turns. Teflon tubes of an inside diameter of 2.0 mm were used. They reported that when the charging ratio was increased, the vapor plugs in the OCHP broke out and only the liquid phase existed. As the operation temperature was high, short liquid and vapor plugs were distributed within the tube. However, the flow pattern in the metal tube was not properly understood because non-metal tubes were also used. Kim et al.(1999) conducted flow visualization experiments according to the heat flux, charging ratio, and inclination angle of the OCHP. The OCHP consisted of a meandering closed structure (4 turns) with a rectangular cross section of 1.5 mm×1.5 mm machined into a brass plate. The working fluid used was ethanol. The detailed flow pattern data were recorded by a high-speed digital camera for each experimental condition. They concluded that the oscillation of vapor bubbles caused by nucleate boiling and vapor oscillation and the departure of small bubbles are considered as the representative flow patterns at the evaporating section and at the adiabatic section, respectively. Miyazaki et al. (1999) also conducted flow visualization experiments of the OCHP with R-142b as the working fluid. The OCHP consisted of 25 channels with a rectangular cross section of 1.0 mm×1.5 mm on a copper plate. They observed the movement phenomena of the oscillation wave of long liquid and

vapor plugs and proposed an analytical model based on these phenomena. However, this model was mostly based on very rough assumptions and simplifications. In fact, the operation mechanism of OCHPs is far from being understood, and there are no reliable data or tools for designing OCHP according to given cooling requirements.

In this study, the flow visualization experiments for both the non-loop and loop type OCHPs of 4 turns (8 channels) and the loop type OCHP of 10 turns (20 channels)) were presented. The detailed flow pattern data were recorded by a high-speed digital camera for each experimental condition to understand exactly the operation mechanism of the OCHP. The design and operation conditions of the OCHP such as turn number, working fluid, and heat flux were varied.

2. Experimental Apparatus and Methods

2.1 Experimental apparatus

The schematic diagram of the experimental apparatus is shown in Fig. 1. It consists of a test section, data acquisition system, heating system, and circulation system of cooling water. The test section was manufactured to the meandering structure with fine flow channels on the surface of a brass plate. The length of the channel was 220 mm. Each channel cross-section was rectangular with a width of 1.5 mm and a height of 1.5 mm. For visualization of the internal flow in the OCHP, the test section was covered with transparent acryl and tightened with bolts. The test sections of the non-loop and loop type of 4 turns (8 channels) and the loop type of 10 turns (20 channels) were used. The detailed specifications of the test section of the loop type of 10 turns were represented in Fig. 2. The data acquisition system was divided into a temperature and pressure measuring system. Each measuring system was composed of a data logger and personal computer. The heating system was an electrical heater plate of which the heat input was adjusted by using a voltage regulator and digital power meter. The circulation system of cooling water was composed of a constant temperature bath and volume-

tric flow meter. The cooling water circulated through the test section, the volumetric flow meter, and the constant temperature bath.
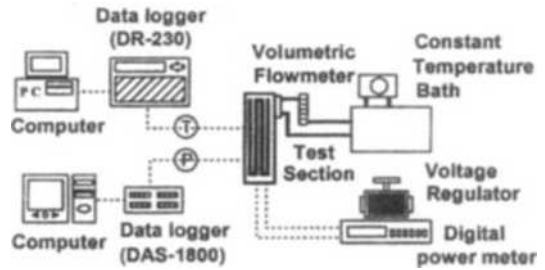

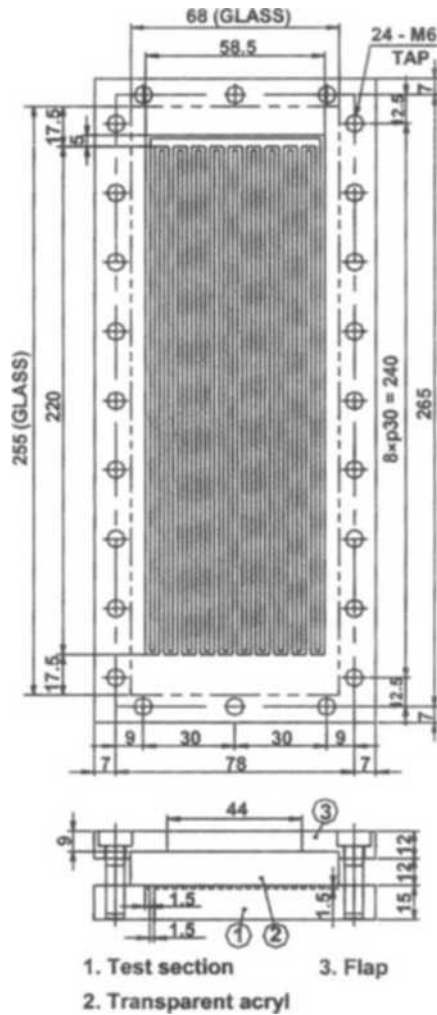**Fig. 1** Schematic diagram of experimental apparatus

1. Test section 　　　3. Flap
2. Transparent acryl

Fig. 2 Specifications of the test section of the loop type of 10 turns

2.2 Experimental methods

The locations of thermocouples for measuring the surface temperature of the test section are shown in Fig. 3. Three holes of a 1.1 mm diameter were perforated into the centre of the test section across and under 1 mm from the bottom of the channel. Three holes were located at the evaporating, adiabatic, and condensing section, respectively. A sheath type thermocouple of a 1.0 mm diameter was inserted and sealed into the hole. To minimize the contact resistance between the perforated hole and the thermocouple, the silicon compound was injected into the gap of the hole. The distance of temperature sensors that were installed at the evaporating and condensing section was 146 mm, and the sensor installed at the adiabatic section was in the middle. Also, the sheath type thermocouples were installed at the inlet and outlet of the cooling water system to measure the temperatures of the circulating cooling water. Copper constantan thermocouples with an experimental uncertainty of
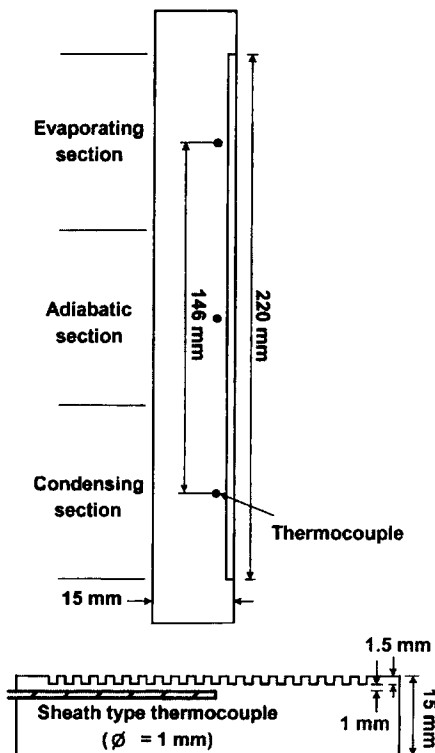
$\pm 0.2°C$ were used for temperature measurements. Each sensor was calibrated to reduce experimental uncertainties and was connected to the data logger (DR-230, Yokogawa Co.).

As shown in Fig. 4, to measure the saturation pressure in the test section, two pressure taps of a 1.0 mm diameter were perforated into a flow channel at the evaporating and condensing section. The pressure sensors (PDCR-961, Druck Co.) with an estimated accuracy of $\pm 0.2\%$ of the full scale (980 kPa) were installed. Pressure data were measured using the DAS-1800 (Keithley Co.) at a steady state. All data were processed using personal computers in real time. The data were measured 5 times at a steady state for 30 minutes and their average was used for data reduction.

The test section was evacuated to 0.0001333 kPa (1×10^{-3} Torr) by using a high vacuum pumping system, which consists of a rotary and diffusion pump. Ethanol and R-142b were used as the working fluids. The charging cylinder (HPG-10,
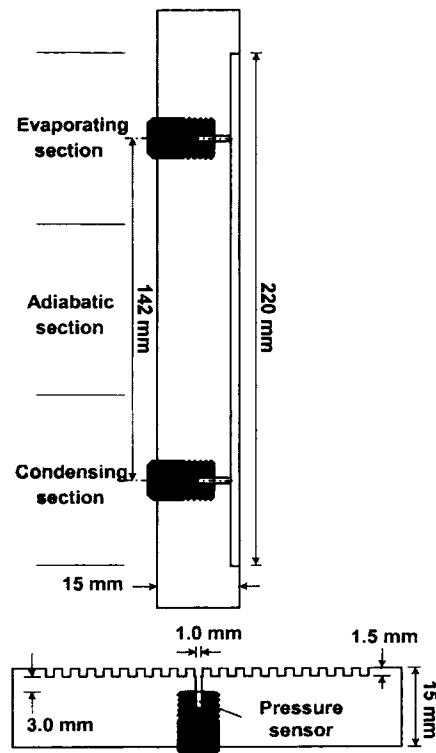
Fig. 3   Locations of thermocouples

Fig. 4   Locations of pressure sensors

Table 1 Test conditions

Specifications		Non-loop type of 4 turns	Loop type of 4 turns	Loop type of 10 turns	
Working fluid		Ethanol	Ethanol	Ethanol	R-142b
Charging ratio (vol.%)	α	40	40	40	40
Input heat flux (W/cm^2)	q	0.45, 0.63, 0.80, 0.97	0.45, 0.63, 0.80, 0.97	0.45, 0.63, 0.80, 0.97	0.3, 0.6, 0.8, 0.9, 1.2
Inclination angle (°)	θ	90	90	90	90

96, Taiatsu Co.) of 10 ml was used to charge the working fluid exactly. A high-speed camera (HAS-200R, Ryokosha Co., Speed of 400 frames/ s, Shutter speed of 1/2000 s) was used. A stroboscope was used as a light source. The speed of the camera used for recording the flow patterns in the OCHP was 0.01 s. The experimental conditions used in this study are represented in the Table 1.

3. Experimental Results and Considerations

3.1 Flow pattern

The OCHP was first evacuated then and filled with working fluid. It was observed that liquid slugs and vapor plugs were randomly distributed in the OCHP. Figure 5 shows the co-existence of liquid slugs and vapor plugs of different lengths in their initial condition in the OCHP, which was placed at the vertical orientation, before heat was applied. When the OCHP was placed in the horizontal orientation, a similar arrangement of liquid slugs and vapor plugs was also observed. This is due to the fact that the surface tension is dominant over the gravitation force. This capillary slug flow is a representative flow pattern in the operation process of the OCHP. Akachi et al. (1994) reported that the flow pattern of liquid and vapor in the OCHP was formed to liquid slugs and vapor plugs and they were distributed irregularly within the tube (of a 0.1~5 mm inner diameter). Rossi et al. (1999) also concluded that this flow pattern existed within a 0.1~3 mm inner diameter range. However, these conditions can differ somewhat from the cross section of the
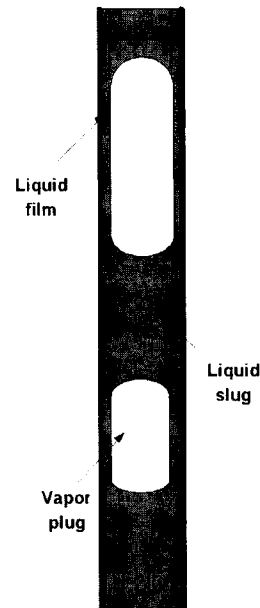
Fig. 5 Capillary slug flow

flow channel, the slip ratio of liquid and vapor, and the properties of working fluid. The flow patterns such as dispersed flow (bubble flow, mist flow), annular flow, churn flow, and wavy flow as well as capillary slug flow are the general flow patterns in the capillary tube of a 1~5 mm inner diameter range (Suo et al., 1964 ; Mishima et al., 1995 ; Kariyasaki et al., 1992 ; Fukano et al., 1990 ; Domianides et al., 1988 ; Coleman et al., 1999).

3.2 Generation and growth process of bubbles

To understand the flow phenomena of the OCHP in detail, the flow pattern was recorded at

the evaporating, adiabatic and condensing sections. The experimental results were represented in series of 10 photographs recorded from 0 s to 0.09 s. Fig. 6 shows the generation and growth process of one bubble at a turn in the evaporating section (loop type OCHP of 4 turns). These
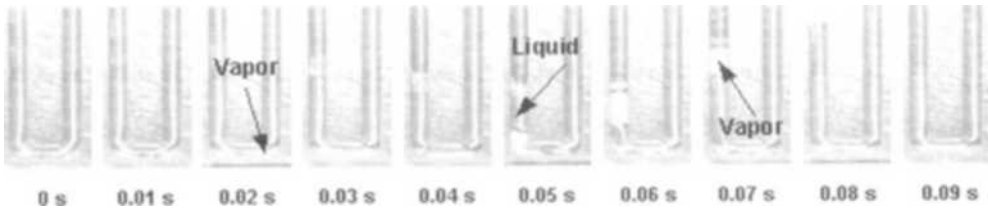

Fig. 6   Generation and growth process of bubble in the evaporating section
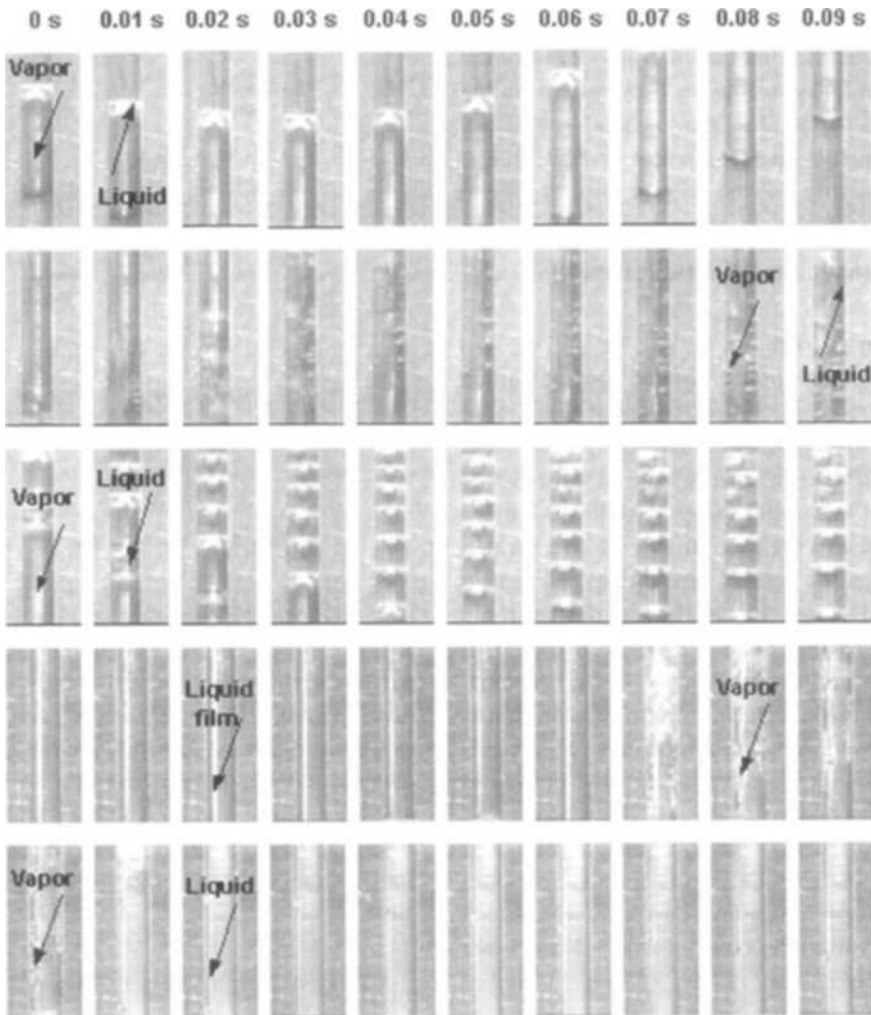[Ethanol, Loop type of 4 turns, $a=40$ vol.%, $\theta=90°$, q$=0.63$ W/cm^2]

Fig. 7   Flow visualization at the evaporating section
[R-142b, Loop type of 10 turns, $a=40$ vol.%, $\theta=90°$, q$=1.2$ W/cm^2]

photographs were taken during the steady state operation of the OCHP at the heat flux of 0.63 W/cm². The generation and growth of bubbles continuously occurred when heat was applied to the evaporating section. This is due to the fact that the internal wall temperature of the channels was higher than the saturated temperature of the working fluid. Bubbles started to generate at the minute cavities in the bottom of the evaporating section by the nucleate boiling process. It took around 0.05 seconds from generation to departure of a bubble in the OCHP. The bubbles grew and coalesced to become vapor plugs and small bubbles were continuously generated. As the bubbles continued to grow in size, liquid and vapor plugs adjacent to the bubbles were propelled toward the condensing section. Because the flow channels were interconnected by U-turns, part of the condensed liquid was returned to the evaporating section due to the movement of the flow within adjacent channels. Another part of the condensed liquid returned to the evaporating section along the channel wall.

Figure 7 shows the series of enlarged photographs of a flow channel at the evaporating section (loop type OCHP of 10 turns). The capillary slug flow at a local point in the evaporating section near the adiabatic section is represented in Fig. 7(a). The oscillation of a long vapor plug and liquid slug was confirmed when condensed liquid was sufficiently supplied to the evaporating section. Figure 7(b) shows the generation process of small bubbles by nucleate boiling in the liquid film (between the vapor plug and channel wall) when the oscillation of the liquid slugs and vapor plugs inside flow channels of the OCHP was active. These bubbles grew quickly and coalesced to become vapor plugs in the evaporating section. Figure 7(c) shows results of the size reduction of bubbles due to the compression operation of the ascending vapor plugs (from the bottom of the evaporating section) and the descending liquid slugs (from the condensing section). As the oscillation of liquid slugs and vapor plugs was very speedy, the average velocity of liquid slugs was around 20 cm/s and the flow pattern changed from the capillary slug flow to a pseudo slug flow

near the annular flow as shown in Fig. 7(d~e). When the images taken were revived slowly after the liquid slug passed, it was observed that small bubbles were generated within the thin liquid film on channel walls. As these small bubbles descend or ascend along channel sides, their size will reach to the size of the channels or they will rupture.

3.3 Flow pattern according to heat flux

Flow pattern was observed with respect to heat flux to find the optimal operation state of the OCHP. Also, the effects of the turn number, the working fluid, and the type of the OCHP (loop type or non-loop type) on flow pattern were examined. Here, the optimal operation state was the state that the oscillation of liquid slugs and vapor plugs was most active. By the very rapid oscillation of vapor plugs and liquid slugs along the flow channels, a pseudo slug flow pattern near the annular flow pattern was formed. The thermal resistance between the surface of channel walls and the working fluid decreased and the heat transfer performance was enhanced.

In the case of the non-loop type OCHP (ethanol, 4 turns), at the heat flux of 0.45 W/cm² the generation and growth of bubbles in the OCHP were an intermittent nucleate boiling process at only some turns among the total flow channels. At the remaining turns of flow channels, bubbles were almost not generated. The bubbles generated by nucleate boiling were only ascended from the bottom to the top of the test section and the oscillation phenomenon was not confirmed. As the heat flux was increased to 0.63 W/cm², small bubbles were generated on the walls (of the channels) in the evaporating section. The bubbles grew and coalesced to become vapor plugs, and the oscillation phenomenon occurred. When the heat flux was increased to 0.8 W/cm² and 0.97 W/cm², the oscillation of liquid slugs and vapor plugs occurred very actively (between the evaporating and condensing sections) and the movement direction of liquid slugs and vapor plugs changed irregularly in each flow channel. A thin liquid film was formed on the walls of the channels due to the very rapid oscillation of

liquid slugs and vapor plugs. The average thickness of the thin liquid film measured at the steady state operation using a microscope was around 100 μm. Bubbles formed within the thin liquid film in the evaporating section separated shortly after they generated from the heated walls. The spaces vacated by the bubbles were immediately filled by the liquid and nucleate boiling process continuously occurred in the evaporating section.

As heat flux was continuously increased to more than 0.97 W/cm^2, the dry-out phenomena occurred and the oscillation of liquid slugs and vapor plugs became slow. This was due to the fact that some of flow channels in the evaporating section started to be filled with vapor. Hence, the supply of working fluid to the evaporating section was reduced. This led to an increase in the surface temperature of the channels. The condensed liquid was evaporated at the superheated walls before it normally arrived to the evapora-

ting section. Only the vapor phase existed in the evaporating section and the oscillation phenomenon did not occur. This state was the operation limit of the OCHP.

Figure 8 shows the flow patterns at the steady state operation of the non-loop type OCHP of 4 turns when the heat flux was 0.8 W/cm^2 (ethanol, the charging ratio of 40 vol.%, and the inclination angle of 90°). In the evaporating section, bubbles were continuously generated on the walls of the channels. These bubbles coalesced to become vapor plugs and the active oscillation phenomenon occurred. In the adiabatic section, the flow pattern was divided into the liquid and vapor phase in the axial direction. The oscillation of liquid slugs and vapor plugs occurred very actively. When long vapor plugs and liquid slugs oscillated in the axial direction, the top part of these vapor plugs was separated to generate short vapor plugs. The flow pattern in the adiabatic
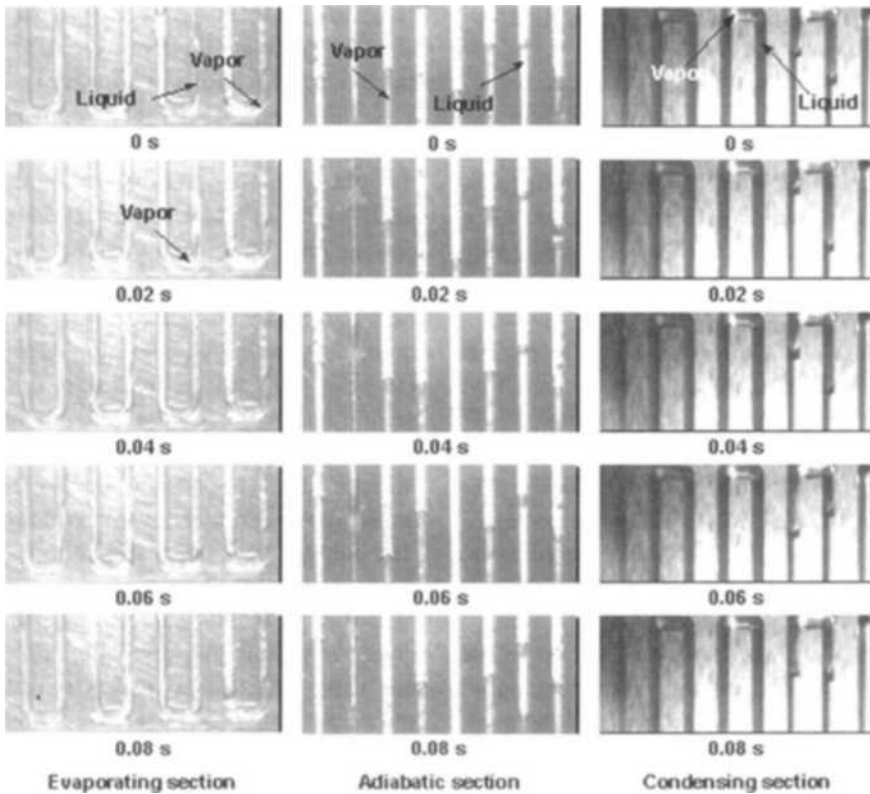

Fig. 8   Flow visualization at each section of the OCHP
[Ethanol, Non-loop type of 4 turns, $\alpha=40$ vol.%, $\theta=90°$, q=0.8 W/cm^2]

section changed to the flow of short vapor-liquid slug-train units. In the condensing section, short vapor plugs reduced in size and disappeared by the condensing process. There was only a small movement of working fluid at the top of each turn and an active movement of working fluid was not observed in this section.

In the case of the loop type OCHP of 4 turns the flow patterns in the evaporating section and adiabatic section were similar to that of the non-loop type OCHP of 4 turns. In the condensing section, because the two ends of the loop type were connected to each other, the circulation of working fluid within the connected channel (of

two branches of the loop type OCHP) occurred as shown in Fig. 9. Also, the oscillation of liquid slugs and vapor plugs in the channels of the loop type was more active than that in the non-loop type. The direction of the circulation (clockwise or anti-clockwise) for the working fluid in the loop type was arbitrary during the steady state operation. The randomness in the direction of the circulation could be attributed to the uneven distribution of liquid slugs and vapor plugs as well as their positions in the OCHP. The effect of the circulation enhanced the capability for the working fluid to transport heat from the evaporating section to the condensing section.
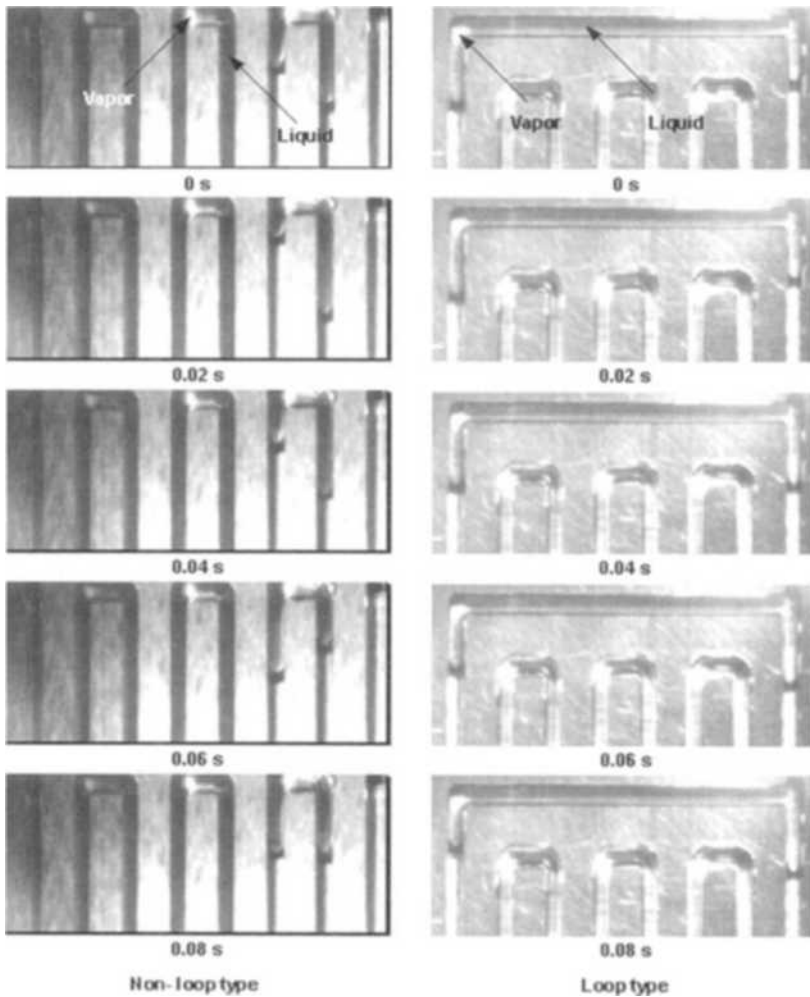

Fig. 9 Difference of the flow pattern between the loop type and the non-loop type OCHP of 4 turns [Ethanol. $a=40$ vol.%, $\theta=90°$, q$=0.8$ W/cm^2]

Figure 10 shows the difference of the flow pattern between the loop type of 4 turns and the loop type of 10 turns. The working fluid used was ethanol at the charging ratio of 40 vol.% and the inclination angle was 90°. When the turn number was increased, the capillary slug flow pattern in which vapor plugs and liquid slugs were well divided, was represented. The flow was very active in the condensing section as heat flux was increased. Also, the circulation of the working fluid was more active at the connected channel. The working fluid in the total flow circulated to one direction in the OCHP. The direction of the circulation of the working fluid was consistent during the steady state operation. The total flow circulated rapidly as well as forming the wave from the left side to the right side or reverse in the OCHP. This flow pattern could not be observed at the loop type OCHP of 4 turns in the same conditions. This was due to the fact that when the turn number was small the degree of freedom of oscillation flow was small. Miyazaki et al.(1999) also confirmed the existence of the oscillation waveform of working fluid by flow visualization experiments using the OCHP of 25 turns. They concluded that the occurrence of the oscillation wave was due to the pressure wave within the OCHP.
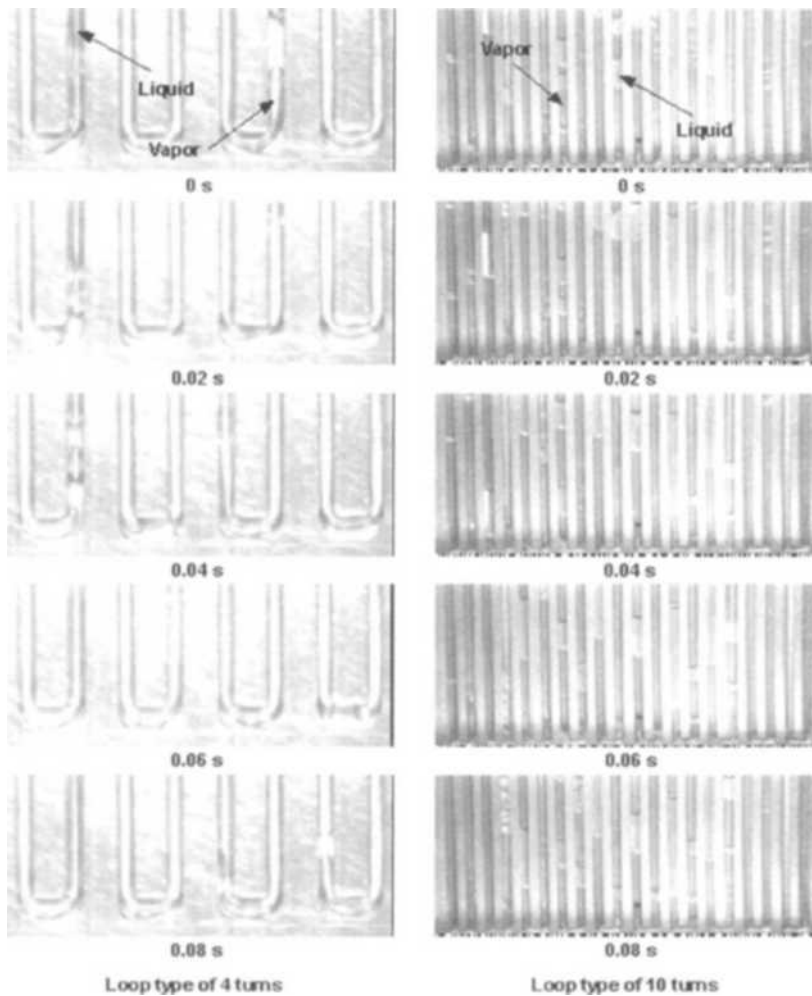

Loop type of 4 turns   Loop type of 10 turns

Fig. 10   Difference of the flow pattern between the loop type of 4 turns and the loop type of 10 turns [Ethanol, α=40 vol.%, θ=90°, q=0.97 W/cm^2]

Figure 11 depicts a rapid waveform by interconnecting the ends of long liquid slugs at each flow channel. The frequency of the oscillation was high when the circulation and oscillation of liquid slugs and vapor plugs were most active. The oscillation frequency was influenced by the heat flux (to the evaporating section). It is noted that the variation of the oscillation frequency corresponded to the oscillation pressure measured in the evaporating section of the test section.

To examine the effect of working fluid on the flow pattern, Ethanol and R-142b were chosen as working fluid in the loop type OCHP of 10 turns (the charging ratio of 40 vol.% and the inclination angle of 90°). The flow pattern of

R-142b was more active than that of ethanol. Generally, in the incipient stage of the low heat
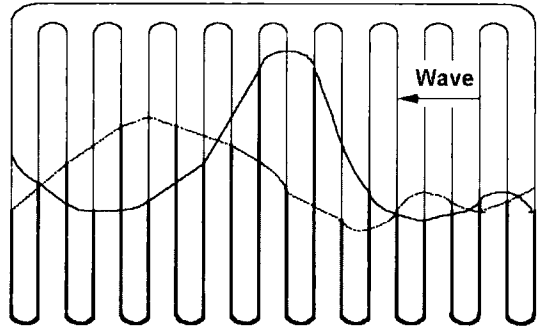

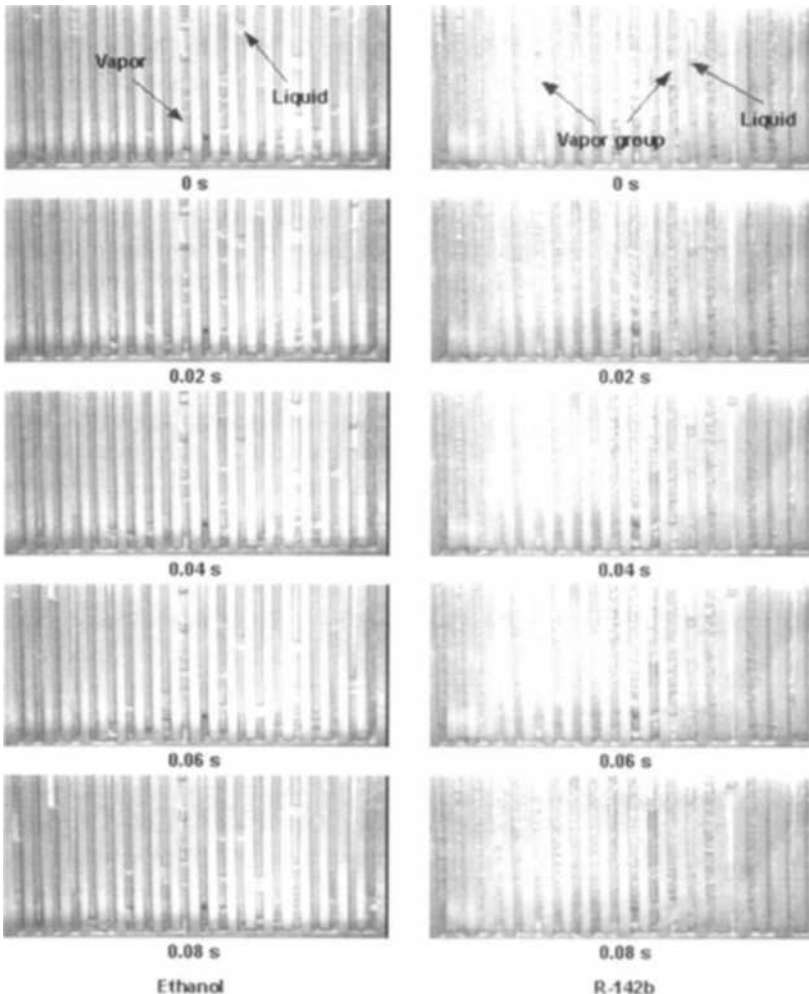**Fig. 11** Schematic diagram of oscillating wave in the OCHP of 10 turns

Fig. 12   Flow patterns according to the working fluid [10 turns, α=40 vol.%, θ=90°, q=0.8 W/cm²]

flux condition, typical case with the working fluid of ethanol, the oscillation phenomenon was not confirmed. As heat flux continuously increased, the oscillation of liquid slugs and vapor plugs in the evaporating section occurred. It differed from the case of ethanol. A large amount of small bubble groups was generated in the liquid film and liquid slugs in the evaporating section as shown in Fig. 12. These small bubbles were explosively expanded and reached the size of the channels. As a result, a long liquid slug was broken up into shorter liquid slugs. Short liquid-vapor slugs moved one after another and the coalescence between short vapor plugs was not detected in the evaporating section. In the adiabatic section, as heat flux was increased, the oscillation of liquid slugs and vapor plugs was very active. The departure of small bubbles at long vapor plugs as well as the departure of short liquid slugs at long liquid slugs was confirmed. In the condensing section, the flow was very active as heat flux was increased and also the circulation of the working fluid was very active at the connected channel. Consequently, the high efficiency of the heat transfer performance of R-142b was achieved as shown in Fig. 13.

The effective thermal conductivity λ_{eff} in Fig. 13 is defined as follows :

$$\lambda_{eff} = \frac{LQ}{A(T_{eva} - T_{cond})}$$

where L is the length from the centre of the evaporating section to that of the condensing section, Q is the heat transfer rate from the evaporating section to the condensing section, A is the total
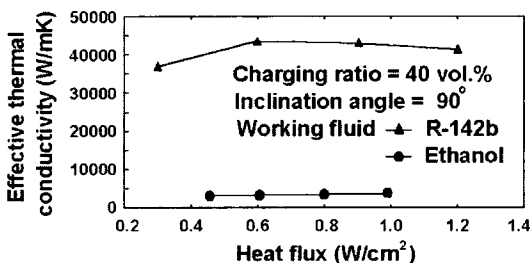

Fig. 13   Effect of the working fluids on the heat transfer performance of the loop type OCHP of 10 turns

cross sectional area of the channels in the OCHP, and T_{eva} and T_{cond} are the mean surface temperatures of the evaporating section and the condensing section, respectively.

The heat released from the condensing section of the test section in the performed experiments was calculated from the measured data of the circulation system of cooling water. The released heat obtained from the experimental data of the cooling water system was in good agreement with the amount of heat added to the evaporating section.

4. Conclusions

(1) The liquid film flow pattern as well as the generation and growth of bubbles were observed in the OCHP. This liquid film flow pattern was formed by the very rapid oscillation of liquid slugs and vapor plugs. The average thickness of the liquid film was around 100 μm. As the heat flux was increased, the small bubbles generated in the liquid film were explosively expanded and coalesced to become vapor plugs in the evaporating section. Its flow pattern was similar to the nucleate boiling regime in pool boiling.

(2) The representative flow pattern in the evaporating section was the oscillation of liquid slugs and vapor plugs based on the generation and growth of bubbles by nucleate boiling. As the oscillation of liquid slugs and vapor plugs were very speedy, the flow pattern changed from the capillary slug flow to a pseudo slug flow near the annular flow. The flow pattern in the adiabatic section was the flow of short vapor-liquid slug-train units. And in the condensing section, the oscillation of liquid slugs and vapor plugs and the circulation of working fluid were observed.

(3) The oscillation flow in the loop type OCHP was more active than that in the non-loop type OCHP due to the circulation of working fluid in the OCHP. When the turn number of the OCHP was increased, the oscillation and circulation of working fluid were more active as well as forming the oscillation wave of long liquid slugs and vapor plugs in the OCHP. The oscillation flow of R-142b as the working fluid was more

active than that of ethanol and the high efficiency of the heat transfer performance of R-142b was achieved.

Acknowledgment

References

Akachi, H., 1994, "Loop type serpentine capillary tube heat pipe," *Proceedings of 71th General Meeting Conference of JSME*, Vol. 3 No. 940-10, pp. 606~611.

Akachi, H., Polasek, F. and Stulc, P., 1996, "Pulsating heat pipes," *Proceedings of 5th Int. Heat Pipe Symposium, Melbourne*, pp. 208~217.

Coleman, J. W. and Garimella, S., 1999, "Characteristics of Two-Phase Flow Patterns in a Small Diameter Round and Rectangular Tubes," *Int. J. of Heat and Mass Transfer*, Vol. 42, pp. 2869~2881.

Domianides, C. A. and Westwater, J. W., 1988, "Two-Phase Flow Patterns in a Compact Heat Exchanger and in Small Tubes," *Proceedings of second U. H. National Conference on Heat Transfer*, Vol. 11, pp. 1257~1268.

Fukano, T., Kariyasaki, A. and Kagawa, M., 1990, "Flow Patterns and Pressure Drop in Isothermal Gas-Liquid Concurrent Flow in a Horizontal Capillary Tube," *JSME(B)*, Vol. 56 No. 528, pp. 174~182.

Gi, K., Sato, F. and Maezawa, S., 1999, "Flow Visualization Experiment on Oscillating Heat Pipe," *36th National Heat Transfer Symposium of Japan*, pp. 659~660.

Hosoda, M., Nishio, S. and Shirakashi, R., 1997, "Bubble-Driven Heat Transport Tube (Flow Pattern and Heat Transport Model)," *34th National Heat Transfer Symposium of Japan*, Vol. 1, pp. 267~268.

Kariyasaki, A., Fukano, T., Ousaka, A. and Kagawa, M., 1992, "Isothermal Air-Water Two-Phase Up and Down flows in a Vertical Capillary tube (1st Report, Flow Pattern and Void Fraction)," *JSME(B)*, Vol. 58 No. 553, pp. 40~46.

Kim, J. S., Lee, W. H., Lee, J. H., Jung, H. S., Kim, J. H. and Jang, I. S., 1999, "Flow Visualization of Oscillating Capillary Tube Heat Pipe," *Proceeding of Thermal Engineering Conference of KSME*, pp. 65~70.

Lee, W. H., Jung, H. S., Kim, J. H. and Kim, J. S., 1999, "Flow Visualization of Oscillating Capillary Tube Heat Pipe," *11th International Heat Pipe Conference*, Tokyo, Japan, Vol. 2, pp. 131~136.

Mishima, K. and Hibiki, T., 1995, "Effect of Inner Diameter on Some Characteristics of Air-Water Two-Phase Flows in Capillary tubes," *JSME(B)*, Vol. 61 No. 589, pp. 99~106.

Miyazaki, Y. and Arikawa, M., 1999, "Visualization of Oscillating heat pipe," *36th National Heat Transfer Symposium of Japan*, pp. 661~662.

Nishio, S., 1997, "Bubble Driven Heat Transport Tubes," *Journal of the Heat Transfer Society of Japan*, Vol. 3 No. 142, pp. 53~56.

Numata, S., Shirakashi, R. and Nishio, S., 1999, "Closed-Loop Heat Transport Tube (Effects of Tube Diameter)," *36th National Heat Transfer Symposium of Japan*, pp. 675~676.

Rossi, L. and Polasek, F., 1999, "Thermal Control of Electronic Equipment by Heat Piped and Two-Phase Thermosyphon," *Proceedings of 11th International Heat Pipe Conference*, Keynote Lecture, Japan.

Suo, M. and Griffith, P., 1964, "Two-Phase Flow in Capillary Tubes," *Journal of Basic Engineering, Transaction of the ASME*, pp. 576~582.

Takahashi, O., Kawara, Z., Serizata, A., Kohno, M., Kakinoki, S. and Akachi, H., 1998, "Visualization of Boiling and Condensation in Capillary Tunnel Type Flat Plate Heat Pipe with Proton Radiography," *35th National Heat Transfer Symposium of Japan*, pp. 529~530.